Am J Transl Res 2018;10(4):1220-1228
www.ajtr.org /ISSN:1943-8141/AJTR0074517

Original Article

Localization of center of intramuscular nerve dense regions in adult anterior brachial muscles: a guide for botulinum toxin A injection to treat muscle spasticity

Shaohua Tang[1], Ming Xiaoming Zhang[2], Shengbo Yang[1]

[1]*Department of Anatomy, Zunyi Medical College, Zunyi, Guizhou Province, People's Republic of China;*
[2]*Department of Molecular and Cellular Biology, Baylor College of Medicine, Houston, Texas, USA*

Received February 13, 2018; Accepted March 16, 2018; Epub April 15, 2018; Published April 30, 2018

Abstract: This study aimed to identify the location and depth of the center of intramuscular nerves dense regions (CINDRs) in anterior brachial muscles. Twelve adult cadavers were used. One side anterior brachial muscles were isolated and subjected to Sihler's staining to show intramuscular nerve dense regions. Then the data was used to localize CINDRs in situ on the same muscles of the contralateral side. The localization method involved dissection and exposure of CINDRs, barium sulfate labeling, body surface reference line design, spiral computed tomography scan, three-dimensional image reconstruction, and Syngo system measurements. The number of CINDRs in coracobrachialis, biceps brachii and brachialis muscle were 3, 2 and 2, respectively. The body surface coordinates for the three CINDRs in coracobrachialis muscle were at 24.22%, 18.89% and 8.15% on the horizontal reference line and 21.37%, 31.78% and 30.07% on the longitudinal reference line. For biceps brachii muscle, they were at 49.68% and 40.28% on the horizontal reference line and 56.60% and 67.63% on the longitudinal reference line. For brachialis muscle, they were at 48.34% and 52.45% on the horizontal reference line and 71.30% and 81.62% on the longitudinal reference line. On cross-sectional planes, the depths of these CINDRs were at 22.81%, 26.76% and 27.99% (coracobrachialis); 14.79% and 17.45% (biceps); 34.03% and 30.26% (brachialis) of section diameters through CINDRs. These results may help to guide the injection of botulinum toxin A for the treatment of spasticity in the anterior brachial muscles and improve treatment efficacy and efficiency.

Keywords: Anterior brachial muscles, muscle spasticity, intramuscular nerve dense regions, spiral computed tomography, target localization

Introduction

The anterior brachial muscle group includes coracobrachialis, biceps brachii and brachialis muscles, which are all innervated by the musculocutaneous nerve. These three muscles may develop spasticity in diseases associated with neuronal injury such as stroke, multiple sclerosis, spinal cord injury, cerebral palsy, and brain trauma [1-3]. Musculocutaneous neurotomy [4, 5], musculocutaneous neurolysis [6-8], and motor point block [9] are commonly used methods for the treatment of the spasticity of these muscles. Recently, injection of botulinum toxin A (BTX-A) to motor endplates to inhibit the release of presynaptic acetylcholine has become an increasingly popular method in treating the spasticity of the anterior brachial muscles [10-12]. Therefore, accurate localization of the motor endplate regions becomes a prerequisite for successful BTX-A injection therapy.

However, the motor endplate staining requires fresh human tissue which is difficult to obtain. As a result, many human muscular motor endplate bands have not been localized accurately, such as coracobrachialis and brachialis muscles. Studies have found that the location of the intramuscular nerve dense region (IDNR) completely co-localize with the motor endplate. For example, the location of the biceps brachii muscle's IDNR, which shapes as an inverted "V", is consistently co-localized with the motor endplate band [13]. Therefore, some investigators began to locate the intramuscular nerve dense regionin place for the motor endplate band [14-

16]. However, take the brachialis muscle as an example, although there is a study of the type of intramuscular nerve branches through Sihler's staining method [17], the location of the intramuscular nerve dense region has not been studies. There was a study about intramuscular nerve branches and their locations through microanatomy dissection, but it did not show intramuscular nerve terminal branches' dense region as shown with the Sihler's staining [18]. For the coracobrachialis muscle, none of the above have been done.

Although there are descriptions about the superioinferior relationship between the nerve branches and the body bony landmarks of the biceps and brachialis, the mediolateral relationship and the puncture depth are still not revealed. The skin surface location of the puncture point is not yet defined, making it difficult for clinical application. It is also worth mentioning that the intramuscular nerve dense region is a region, not a point. Therefore, inaccurate localization does not help to achieve a satisfactory result in BTX-A therapy for muscle spasticity. It has become necessary to obtain more accurate anatomical information of the INDRs.

This study adopted a modified Sihler's staining method to reveal the IDNRs and the centers of INDRs (CINDRs) on isolated muscles and apply this knowledge to the comparable contralateral muscles in situ through barium sulfate labeling, spiral CT scanning, and three-dimensional image reconstruction. We then mapped out the CINDRs of the in situ anterior brachial muscles in relationship to bony landmarks and the depth underneath the skin. We hope that this work can provide application guidance for the BTX-A injection and to improve the efficacy and efficiency of muscle spasticity treatment.

Materials and methods

Specimen and ethics

A total of 12 adult cadavers (7 men, 5 women) were collected. There were no history of neuromuscular disease, nor chest and upper limb deformity. The bodies were fixed with formaldehyde and the anatomical position was maintained. This experiment was carried out under the consent of our school ethics committee.

Gross anatomy and measurement

Cadavers were placed insupine position. A longitudinal skin incision was made from the acromion to 1 cm posterior to the lateral epicondyle of humerus. A transverse skin incision was made from the acromion to 1 cm above the jugular notch. A third skin incision was done 5 cm below the connecting line from medial epicondyle to lateral epicondyle of humerus. After reflecting the skin and subcutaneous fat, we incised the attachment of pectoralis major to the humerus and reflect it medially. The attachments of all three anterior brachial muscles were dissected and exposed. These muscles were carefully separated from the bone surface and completely removed from one side (6 left and 6 right, of all 12 cadavers). Muscles were measured with a vernier caliper for their length (from the nearest origin to the farthest insertion) and width (from medial to lateral).

Reference line design

In order to map out the positions of the CINDRs in each muscle on a two-dimensional plane, i.e., superioinferior and mediolateral, we established a coordinate system by using the bony landmarks in the upper limb. The acromion (A), lateral epicondyle of humerus (B), medial epicondyle of humerus (C), and the lowest point of jugular notch (D) were used to design reference lines. The connecting line, which is slightly curved on skin surface, between point A and B is defined as the longitudinal reference line (L). Two body surface horizontal reference lines (H) were designed as H_1 connecting A to D and H_2 connecting B to C, both of which were slightly curved on skin surface. H_1 was used for coracobrachialis muscle and H_2 for brachialis and biceps brachii muscles (**Figure 1A**).

Sihler's staining method showed intramuscular nerve dense regions

Fat and fascia were trimmed off from the muscle specimens harvested for Sihler's staining process. Briefly, specimens were soaked in a solution containing 3% hydroxide and 0.2% peroxide for 4 weeks; decalcified 4 weeks in Sihler's I solution (1 portion glacial acetic acid, 2 portions of glycerin, and 12 portions of 1% chloral hydrate); stained in Sihler's II solution (1 Ehrlich dyeing liquid, 2 copies of glycerin, 12 copies of 1% chloral hydrate) for 4 weeks;

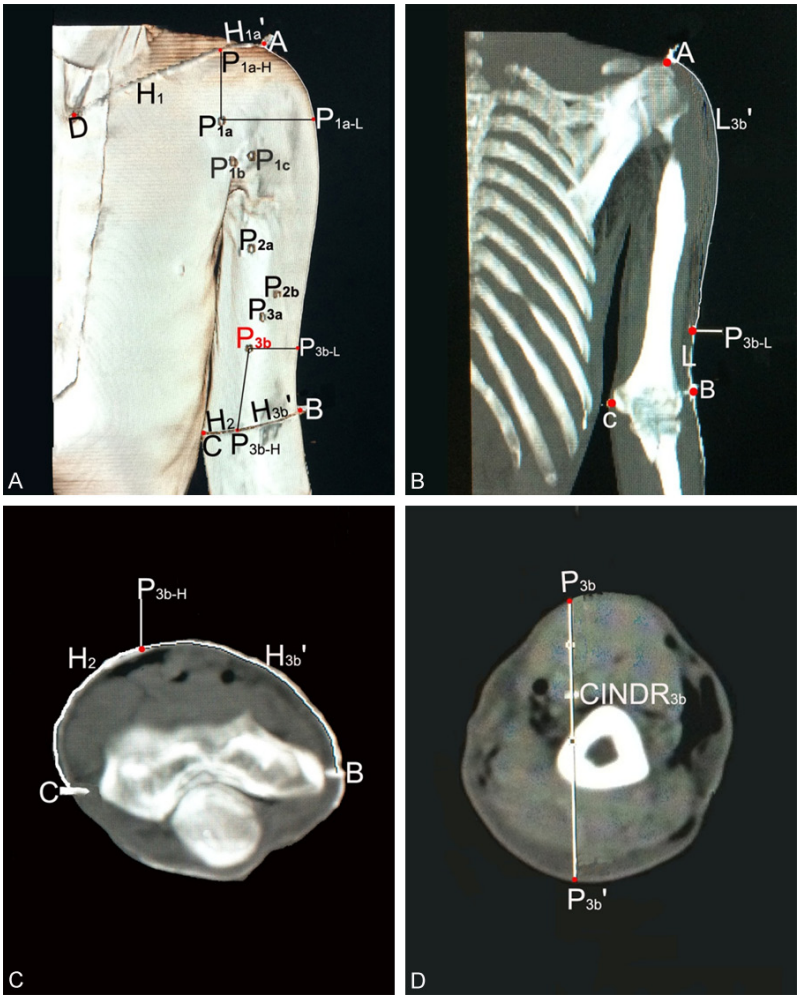

Figure 1. CT imaging of the CINDR localization of the anterior brachial muscles of the left arm. A. 3D reconstruction image from spiral CT showing body surface projection positions of CINDRs and reference lines. P_{1a}, P_{1b} and P_{1c} were the body surface projection points for CINDRs of coracobrachialis, P_{2a} and P_{2b} of the short head and the long head of biceps brachii, P_{3a} and P_{3b} of brachialis. AB=L, A-P_{1a-L}=L_{1a}', A-P_{3b-L}=L_{3b}'; AD=H_1, BC=H_2, A-P_{1a-H}=H_{1a}', B-P_{3b-H}=H_{3b}'. B. The length of L and L_{3b}' were measured on the coronal section through AB line (brachialis muscle as an example); C. The length of H_2 and H_{3b}' were measured on the cross section through H_2 line; D. The depth of $CINDR_{3b}$ was measured on the cross section through P_{3b}.

decolorized in Sihler's I solution 3~20 h; neutralized in 0.05% lithium carbonate solution for 2 hours; and soaked in steps in gradient glycerine (40%, 60%, 80%, 100%) for 1 week to obtain transparency. The intramuscular distribution of nerve branches was carefully observed under X-ray and the distribution patterns were hand drawn. The length and width of INDRs in each muscle were measured with a vernier caliper and calculated for its area of distribution. The position of CINDRs in each muscle were located as a percentile to the muscle length and width.

Spiral CT localization of CINDR

According to our previous published CINDR localization method [16], anterior arm group muscles were carefully dissected and exposed on the contralateral side, i.e., the contralateral side of where muscles were removed for Sihler staining. Muscles were left in situ and measured for length, width and thickness using a vernier caliper. The Sihler's staining results obtained from the muscles removed previously on the contralateral limb were used as a reference to find the corresponding positions of the CINDRs of the muscles in situ. Barium sulfate (Shandong Jiashuo Radiation Protection Engineering Co. Ltd., China) mixed with 801 glue (Shanghai Micro Spectrum Chemical Technology Services Co., China) were injected into the location of measured CINDRs and the dissection was then sutured back to normal anatomical position. A needle was inserted at each body surface bony landmarks and the needles were connected with silk threads soaked with barium sulfate. These silk threads were sewn to skin surface representing the body surface reference lines of H and L. Specimens were then scanned with the 16-row spiral computed tomography (Siemens, Germany). Three-dimensional image reconstruction was done based on the CT scan data. The barium sulfate labeled spots that first appeared in a distal-to-proximal cross section plane was defined as a CINDR. Using the same indicator lamp, with the aid of spiral CT scanning, a needle was inserted through skin perpendicular to the coronal plane toward the CINDR. The needle insertion point was defined as projection

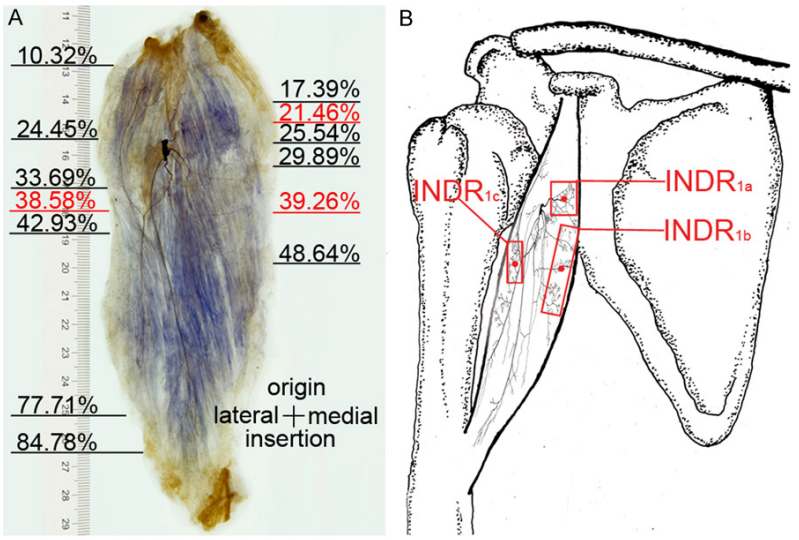

Figure 2. The intramuscular nerves distribution pattern and the position of CINDRs in the right coracobrachialis muscle. A. Sihler's staining showed the distribution of intramuscular nerve. B. A schematic drawing showing the intramuscular position of INDRs and CINDRs. The red boxes are INDRs, and the red dots represent CINDRs.

Table 1. The percentage location of CINDR on muscle length and width

CINDR	Location of CINDR on muscle length (%)	Location of CINDR on muscle width (%)
$CINDR_{1a}$	21.46±0.56	34.84±0.46
$CINDR_{2b}$	39.26±1.15	28.81±0.25
$CINDR_{3c}$	38.58±0.78	81.35±0.75
$CINDR_{2a}$	40.67±0.35	29.07±0.33
$CINDR_{2b}$	55.93±0.84	70.12±0.74
$CINDR_{3a}$	33.78±0.44	68.63±0.39
$CINDR_{3b}$	45.27±0.76	21.96±0.34

point (P) of CINDR and was considered as the body surface puncture point for the specific CINDR. According to Sihler's staining results, there were 3 CINDRs in coracobrachialis, 2 in biceps brachii and 2 in brachialis muscles respectively. The CINDRs in coracobrachialis were named as $CINDR_{1a}$, $CINDR_{1b}$ and $CINDR_{1c}$, the P points were P_{1a}, P_{1b}, P_{1c}. Similarly, the CINDRs in biceps brachii were named as $CINDR_{2a}$ and $CINDR_{2b}$ and the P points as P_{2a} and P_{2b}. The CINDRs in brachialis were $CINDR_{3a}$ and $CINDR_{3b}$ with the P points as P_{3a} and P_{3b}. Following repeated CT scanning, three-dimensional image reconstruction was carried out and a curve measuring tool was used under the Syngo system (Siemens, Germany). The total lengths of L and H were measured along the coronal and cross-skin surfaces, respectively. The intersection point of the horizontal line and line L through P was designated as P_L, the length between the point A and P_L was designated as L'. For coracobrachialis, the intersection point of the vertical line and line AD (H_1) through P was designated as P_{1H}, A-P_{1H}= H_1'. For the biceps brachii and brachialis, the intersection point of the straight line parallel to the axis of the arm and line BC (H_2) through P was designated as P_{2H} or P_{3H}, the length between point B and P_H was designated as H_2' or H_3' (**Figure 1A-C**). The H'/H × 100% and L'/L × 100% were calculated to determine the percentage position of the CINDRs on body surface. In the cross-sectional images, from P point, through CINDR, projecting to the skin surface of the opposite side created a skin surface point designated as P'. Lines P-CINDR and PP' were measured using a linear tool (**Figure 1D**). P-CINDR/PP' × 100% was calculated in order to determine the percentage puncture depth. After the above in situ localization procedure, the 12 sets of in situ anterior brachial muscles were removed and subjected to Sihler's staining to verify the intramuscular nerves distribution pattern and position of CINDR and to compare with those on the contralateral sides.

Statistical processing

The experimental results were expressed as a percentage of total length of muscles or on reference lines to eliminate the differences of body weight and height between individuals. The comparison between two sides was calculated with paired *t* test, and the level of significance was 0.05.

Results

Localization of INDRs and CINDRs on isolated muscles

The coracobrachialis branch of musculocutaneous nerve entered the muscle from deep sur-

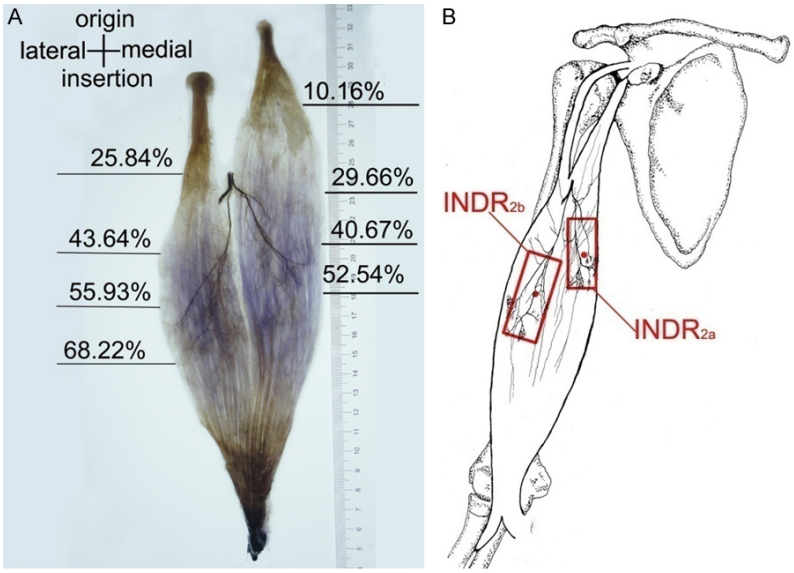

Figure 3. The intramuscular nerve distribution pattern and the position of CINDRs in the right biceps brachii muscle. A. Sihler's staining showing the distribution of intramuscular nerve branches. B. A schematic drawing showing the intramuscular position of INDRs and CINDRs. The red boxes are INDRs, and the red dots represent CINDRs.

face at 24.45% of muscle length and traveled to the center of the muscle and then, often divided into 5 primary nerve branches. Three primary branches traveled inferomedially, projected abundant arborized branches, anastomosed with each other into a network, and distributed to the muscle fibers on the medial half of the muscle. There were two intramuscular nerve dense regions ($INDR_{1a}$, $INDR_{1b}$) at 17.39%~25.54% and 29.89%~48.64% level of muscle length respectively covering two areas about (6.54±0.22) and (13.15±0.47) cm^2. The other two primary branches traveled inferolaterally to the lateral half of the muscle. One of them divided into 2 secondary branches reaching the proximal 10.32% and the distal 77.71% level of muscle length respectively. There was 1 nerve dense region ($INDR_{1c}$) at 33.69% to 42.93% of muscle length and it covers an area of (4.15±0.37) cm^2. The other primary branch traveled more distal reaching 84.78% of muscle length. The positions of above three INDRs were shown in **Figure 2** and **Table 1**.

The musculocutaneous nerve extended two branches to biceps brachii from deep surface at 25.84% of the muscle length into the short head and the long head patterned like an inverted V shape. Four primary branches come off from the short head branch at 29.66% of the muscle length. One of them on the medial of muscle turned superomedially and reached 10.16% level of muscle length and innervated the muscle fibers of short head upper part. The other three primary branches traveled inferomedially, with one thicker branch projected abundant arborized branches along the way anastomosing with the other two primary branches and forming an oblique intramuscular nerve dense region ($INDR_{2a}$) at 29.66%~52.54% of muscle length occupying an area of (21.73±0.48) cm^2. The long head branch divided into three primary branches at 43.64% of muscle length running inferolaterally giving off many arborized branches. It reached 68.22% of muscle length. There was one intramuscular nerve dense region ($INDR_{2b}$) formed with an area of (21.83±0.53) cm^2. The $INDR_{2a}$ was located higher than $INDR_{2b}$. The location of these CINDRs were shown in **Figure 3** and **Table 1**.

The nerve branch for brachialis entered the muscle at medial 18.24% of muscle length. It divided into to two primary branches at 27.02% muscle length. The lateral primary branch sent three secondary branches going laterally and sending many arborized branches, which formed an intramuscular nerve dense region ($INDR_{3a}$) at 19.59%~47.29% muscle length occupying an area of (18.48±0.39) cm^2. The medial primary branchal so sent three secondary branches at 32.43% muscle length with the middle one traveled the furthest to 87.83% of muscle length. These nerve branches formed an intramuscular nerve dense region ($INDR_{3b}$) with an area of (6.48±0.27) cm^2. $INDR_{3a}$ was located higher than $INDR_{3b}$ and their coordinates on muscle length and width are shown in **Figure 4** and **Table 1**.

Spiral CT localization of the anterior brachial muscle CINDRs

The projection positions of body surface and depths of $CINDR_{1a}$, $CINDR_{2b}$ and $CINDR_{3c}$ in cor-

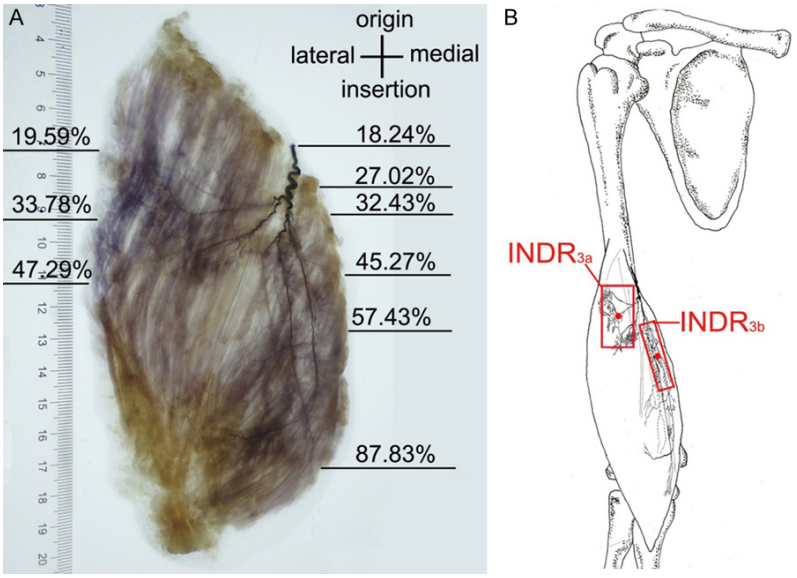

Figure 4. Intramuscular nerve distribution pattern and positions of CINDRs in the right brachialis muscle. A. Sihler's staining showing the distribution of intramuscular nerve branches. B. A schematic drawing showing the intramuscular positions of INDRs and CINDRs. The red boxes are INDRs, and the red dots represent CINDRs.

Table 2. The location of P_H and P_L on Line H and L and the depth of CINDRs on PP'

CINDR	Location of P_H on H (%) H'/H (%)	Location of P_L on L (%) L'/L (%)	Depth of CINDR (%) P-CINDR/PP' (%)
$CINDR_{1a}$	24.22±1.49	21.37±2.48	22.81±1.59
$CINDR_{1b}$	18.89±1.49	31.78±2.32	26.76±1.32
$CINDR_{1c}$	8.15±1.14	30.07±1.12	27.99±2.04
$CINDR_{2a}$	49.68±2.03	56.60±3.35	14.79±1.35
$CINDR_{2b}$	40.28±2.58	67.63±3.29	17.45±1.28
$CINDR_{3a}$	48.34±3.25	71.30±3.06	34.03±1.10
$CINDR_{3b}$	52.45±3.47	81.62±4.70	30.26±3.14

acobrachialis, $CINDR_{2a}$ and $CINDR_{2b}$ in biceps brachii, and $CINDR_{3a}$ and $CINDR_{3b}$ in brachialis muscles on body surface were shown in **Figure 1** and **Table 2**. Here, we used $CINDR_{3b}$ of brachialis as a representative demonstration (**Figure 1A-D**). The positions of the CINDRs between the left and the right were compared and there was no statistical significance, P=0.09.

Discussion

Muscle spasticity is one of the common clinical manifestations as results of many central nervous system injuries. Muscle spasticity often occur in upper limb flexor and lower limb extensor, defined as "Wernicke-Mann" posture [12]. The elbow joint flexors are at a high risk of muscle spasticity, in which patients usually show elbow flexion with difficulties in stretching the arm, in dressing themselves, and in reaching objects [2]. Therefore, relieving the muscle spasticity and increasing the mobility of the elbow joint are the focuses of rehabilitation medicine. However, when using botulinum toxin A injection to treat muscle spasticity, the accuracy for blocking targets is still an issue although the procedure can be assisted with palpation, electromyography, electrical stimulation, and ultrasound. There are various limitations associated with these assisting methods and as a result, inaccurate blocking injection creates unavoidable exploratory skin punctures bringing pain and unnecessary complications to patients. Therefore, it is necessary to obtain more detailed information about the anatomical localization of the injection targets, i.e., INDRs and CINDRs.

Previous studies have shown that the motor endplate of biceps brachiiis an inverted "V" in shape and is located together with the intramuscular nerve dense region. The medial part of this motor endplate band is located at 7 cm above the olecranon, the lateral part at 8 cm above the olecranon, and the central part at 11 cm above the olecranon [13]. However, in this study the measurements about the distances between the position of the motor endplate band and the bony landmarks were expressed as absolute value, which is not necessarily accurate when applying to individuals with different height and body weight. Also, the 3-dimensional relationship between the endplate band and the bony landmarks was not

revealed, instead, only muscle origins and insertions were described. It is difficult for clinicians to exactly locate the injection target from the body surface based on this data. Moon et al located the position of the motor point in the biceps by using standard electrophysiology approach from body surface but he did not reveal the puncture depth. Another study revealed the intramuscular nerve branch dense regions of the biceps and brachialis via microanatomy and established their three-dimensional relationship but did not indicate body surface puncture location [18]. All of these studies measured distances between the blocking target and the bony landmarks in a straight line whereas the body surface is actually curved. Therefore, results from these research data may not guide actual operation accurately. The results of our study are different from those of the above studies because we took into consideration of body surface curvature in our measurement.

Our results suggest that when clinicians need to locate the CINDRs of the coracobrachiali, they should measure the curved distance between the acromion and the lowest point of jugular notch using a tape measure placed close to skin. Then, at the corresponding percentage position draw a vertical line downward. Another body surface curved line should be drawn from the acromion to the lateral epicondyle of humerus. A horizontal line at the corresponding position can be also produced. The intersection of the vertical and horizontal lines on body surface is the skin puncture point (P). Using a pelvis measuring instrument, starting from P point through the coronal plane to the opposite side, the PP' line can be measured. Calculated corresponding percentage will allow one to obtain the puncture depth. Similar methods can be used to localize the CINDRs of biceps brachii and brachialis muscles.

The target of BTX-A treatment is the motor endplate and therefore, its treatment efficacy depends on the distance between the needle tip and the endplate. Because the BTX-A injection is a dose-dependent nerve blocking process, the reagent diffuses immediately within a few centimeters near the tip of the needle once injected into the muscle [19]. Therefore, our experiment was aimed at CINDR as the target location with a hope that the drug would diffuse and infiltrate the surrounding nerve branches. However, there are 2~3 INDRs in these muscles and they are not located close to each other. This indicates that multiple point injections may produce better effects. If BTX-A injection site deviates 5 mm from the motor endplate, the antispasmodic effect will be reduced by 50% [20]. Although increasing BTX-A dosage within a certain range may improve the therapeutic effect, regional muscle fibrosis and excessive muscle relaxation may happen when long-term and high doses are used. In addition, repeated BTX-A injections bring pain to patients and can also lead to ineffective or invalid BTX-A treatment [21]. Therefore, appropriate amount of BTX-A should be injected into the effective part of the target muscle (INDR). Studies have shown that 1 unit BTX-A can infiltrated 1.5~3 cm^2 tissue area, 2.5~5 units are dispersed to 4.5 cm^2 [16, 19]. In the cases of coracobrachialis, biceps brachii, and brachialis muscle spasticity, the required BTX-A dose are (40±5.0), (111.7±48.0) and (4.1±23.2) 5 units respectively [22, 23]. However, based on the calculations of INDR areas in our results, dosages needed for BTX-A injected into the CINDR are 14 to 28 units for coracobrachialis, 24 to 48 units for biceps brachii, and 14 to 28 units for brachialis muscles. This will largely reduce the injection dose, therefore the cost for the medicine, and greatly increase the effects of treatment.

In summary, this study showed that intramuscular INDRs of the anterior brachial muscles can be revealed through modified Sihler's staining method. They can be also localized in situ via barium sulfate marking, spiral CT scanning, and 3-D image reconstruction. Body surface bony landmarks help to design reference lines, which can be conveniently used to localize the CINDRs on body surface as well as to measure the puncture depth. The curved skin surface reference lines and the percentage calculations on these lines help to increase measurement accuracy and feasibility. It can provide scientific guidance to improve the efficiency and efficacy in treating the anterior brachial muscle spasticity. Nevertheless, we still recommend that auxiliary methods such as combined electrical stimulator, ultrasound, or electromyography are used in clinical application in order to further reduce the pain caused by exploratory punctures. After all, the efficacy of these results still needs to be confirmed by clinical application.

Acknowledgements

The authors would like to acknowledge Shuangjiang Hu and Xufeng Tian for their excellent technical assistance and use of their spiral CT laboratory. This work was supported by the National Natural Science Foundation of China (No. 31660294, 31540031) and the Provincial Natural Science Joint Foundation of Guizhou (No. LH-2015-7528).

Disclosure of conflict of interest

None.

Address correspondence to: Shengbo Yang, Department of Anatomy, Zunyi Medical College, 6 University West Road, Xinpu New Developing Areas, Zunyi 563099, Guizhou Province, People's Republic of China. Tel: +8615885627077; Fax: +8608528-609666; E-mail: yangshengbo8205486@163.com

References

[1] Dong Y, Wu T, Hu X, Wang T. Efficacy and safety of botulinum toxin type A for upper limb spasticity after stroke or traumatic brain injury: a systematic review with meta-analysis and trial sequential analysis. Eur J Phys Rehabil Med 2017; 53: 256-267.

[2] Picelli A, Vallies G, Chemello E, Castellazzi P, Brugnera A, Gandolfi M, Baricich A, Cisari C, Santamato A, Saltuari L, Waldner A, Smania N. Is spasticity always the same? An observational study comparing the features of spastic equinus foot in patients with chronic stroke and multiple sclerosis. J Neurol Sci 2017; 380: 132-136.

[3] Korzhova JE, Chervyakov AV, Poydasheva AG, Kochergin IA, Peresedova AV, Zakharova MN, Suponeva NA, Chernikova LA, Piradov MA. The application of high-frequency and iTBS transcranial magnetic stimulation for the treatment of spasticity in the patients presenting with secondary progressive multiple sclerosis. Vopr Kurortol Fizioter Lech Fiz Kult 2016; 93: 8-13.

[4] Cambon-Binder A, Leclercq C. Anatomical study of the musculocutaneous nerve branching pattern: application for selective neurectomy in the treatment of elbow flexors spasticity. Surg Radiol Anat 2015; 37: 341-348.

[5] Garland DE, Thompson R, Waters RL. Musculocutaneous neurectomy for spastic elbow flexion in non-functional upper extremities in adults. J Bone Joint Surg Am 1980; 62: 108-112.

[6] Lee DG, Jang SH. Ultrasound guided alcohol neurolysis of musculocutaneous nerve to relieve elbow spasticity in hemiparetic stroke patients. Neuro Rehabilitation 2012; 31: 373-377.

[7] Kong KH, Chua KS. Neurolysis of the musculocutaneous nerve with alcohol to treat post-stroke elbow flexor spasticity. Arch Phys Med Rehabil 1999; 80: 1234-1236.

[8] Keenan MA, Tomas ES, Stone L, Gerstén LM. Percutaneous phenol block of the musculocutaneous nerve to control elbow flexor spasticity. J Hand Surg Am 1990; 15: 340-346.

[9] Buchanan TS, Erickson JC. Selective block of the brachialis motor point. An anatomic investigation of musculocutaneous nerve branching. Reg Anesth 1996; 21: 89-92.

[10] Esquenazi A, Mayer N, Garreta R. Influence of botulinum toxin type A treatment of elbow flexor spasticity on hemiparetic gait. Am J Phys Med Rehabil 2008; 87: 305-310.

[11] Lim YH, Choi EH, Lim JY. Comparison of effects of botulinum toxin injection between subacute and chronic stroke patients: a pilot study. Medicine (Baltimore) 2016; 95: e2851.

[12] Nam HS, Park YG, Paik NJ, Oh BM, Chun MH, Yang HE, Kim DH, Yi Y, Seo HG, Kim KD, Chang MC, Ryu JH, Lee SU. Efficacy and safety of NABOTA in post-stroke upper limb spasticity: a phase 3 multicenter, double-blinded, randomized controlled trial. J Neurol Sci 2015; 357: 192-197.

[13] Amirali A, Mu L, Gracies JM, Simpson DM. Anatomical localization of motor endplate bands in the human biceps brachii. J Clin Neuromuscul Dis 2007; 9: 306-312.

[14] An XC, Lee JH, Im S, Lee MS, Hwang K, Kim HW, Han SH. Anatomic localization of motor entry points and intramuscular nerve endings in the hamstring muscles. Surg Radiol Anat 2010; 32: 529-537.

[15] Yang F, Zhang X, Xie X, Yang S, Xu Y, Xie P. Intramuscular nerve distribution patterns of anterior forearm muscles in children: a guide for botulinum toxin injection. Am J Transl Res 2016; 8: 5485-5493.

[16] Yang S, Hu S, Li B, Li X. Localization of nerve entry point and intramuscular nerve dense regions as targets to block brachioradialis muscle spasticity. Int J Clin Exp Med 2017; 10: 11912-11920.

[17] Won SY, Cho YH, Choi YJ, Favero V, Woo HS, Chang KY, Hu KS, Kim HJ. Intramuscular innervation patterns of the brachialis muscle. Clin Anat 2015; 28: 123-127.

[18] Lee JH, Kim HW, Im S, An X, Lee MS, Lee UY, Han SH. Localization of motor entry points and terminal intramuscular nerve endings of the musculocutaneous nerve to biceps and brachialis muscles. Surg Radiol Anat 2010; 32: 213-220.

[19] Borodic GE, Ferrante R, Pearce LB, Smith K. Histologic assessment of dose-related dffusion and muscle fiber response after therapeutic botulinum A toxin injections. Mov Disor 1994; 9: 31-39.
[20] Parratte B, Tatu L, Vuillier F, Diop M, Monnier G. Intramuscular distribution of erves in the human triceps surae muscle: anatomical bases for treatment of spastic drop foot with botulinum toxin. Surg Radiol Anat 2002; 24: 91-96.
[21] Ghasemi M, Salari M, Khorvash F, Shayganne-jad V. A literature review on the efficacy and safety of botulinum toxin: an injection in post-stroke spasticity. Int J Prev Med 2013; 4 Suppl 2: S147-58.
[22] Chinese ARM. Chinese guidebook for the treatment of adult limb spasticity by botulinum toxin injection. Chin J Rehabil Med 2015; 30: 81-110.
[23] Horimoto Y, Inagaki A, Yoshikawa M, Kanbe K, Tanaka H, Ando R, Hibino H, Tajima T, Fukagawa K, Kabasawa H. Therapeutic outcome of onabotulinum toxin type A in patients with upper limb spasticity. Rinsho Shinkeigaku 2015; 55: 544-549.